Composites Part B 95 (2016) 225–239

Contents lists available at ScienceDirect

Composites Part B

journal homepage: www.elsevier.com/locate/compositesb

# Shear strengthening of full-scale RC T-beams using textile-reinforced mortar and textile-based anchors

Zoi C. Tetta [a], Lampros N. Koutas [b], Dionysios A. Bournas [c, *]

[a] Department of Civil Engineering, University of Nottingham, NG7 2RD, Nottingham, UK
[b] Department of Civil and Structural Engineering, University of Sheffield, Sir Frederick Mappin Building, Mappin Street, Sheffield, S1 3JD, UK
[c] European Laboratory for Structural Assessment, Institute for the Protection and Security of the Citizen, Joint Research Centre, European Commission, T.P. 480, I-21020 Ispra (VA), Italy

ARTICLE INFO

*Article history:*
Received 19 January 2016
Received in revised form
21 March 2016
Accepted 25 March 2016
Available online 2 April 2016

*Keywords:*
A. Fabrics/textiles
A. Carbon fibre
A. Glass fibres
B. Debonding
Textile anchors

ABSTRACT

This paper presents a study on the effectiveness of TRM jacketing in shear strengthening of full-scale reinforced concrete (RC) T-beams focussing on the behaviour of a novel end-anchorage system comprising textile-based anchors. The parameters examined in this study include: (a) the use of textile-based anchors as end-anchorage system of TRM U-jackets; (b) the number of TRM layers; (c) the textile properties (material, geometry); and (d) the strengthening system, namely textile-reinforced mortar (TRM) jacketing and fibre-reinforced polymer (FRP) jacketing for the case without anchors. In total, 11 full-scale RC T-beams were constructed and tested as simply supported in three-point bending. The results showed that: (a) The use of textile-based anchors increases dramatically the effectiveness of TRM U-jackets; (b) increasing the number of layers in non-anchored jackets results in an almost proportional increase of the shear capacity, whereas the failure mode is altered; (c) the use of different textile geometries with the same reinforcement ratio in non-anchored jackets result in practically equal capacity increase; (d) TRM jackets can be as effective as FRP jackets in increasing the shear capacity of full-scale RC T-beams. Finally, a simple design model is proposed to calculate the contribution of anchored TRM jackets to the shear capacity of RC T-beams.



## 1. Introduction and background

The issue of upgrading existing structures has been of great importance over the last decades due to their deterioration; ageing, environmental induced degradation, lack of maintenance or need to meet the current design requirements. Replacing the deficient concrete structures in the near future with new is not a viable option as it would be prohibitively expensive. For this reason a shift from new construction towards renovation and modernisation has been witnessed in the European construction sector, between 2004 and 2013, with practically 50% of the total construction output being renovation and structural rehabilitation (i.e. €305bn turnover on rehabilitation and maintenance works in EU27 for 2012, see www.fiec.eu). To address cost effectiveness, a new composite material, namely textile-reinforced mortar (TRM) has been proposed for structural retrofitting [1,2], over the last decade.

TRM combines advanced fibres in form of textiles (with open-mesh configuration) with inorganic matrices, such as cement-based mortars. TRM is a low cost, friendly for manual workers, fire resistant, and compatible to concrete and masonry substrates material which can be applied on wet surfaces or at low temperatures. For all these reasons, using TRM will progressively become more attractive for the strengthening of existing concrete and masonry structures than the widely used fibre-reinforced polymers (FRPs). TRM system has been investigated as strengthening system of reinforced concrete (RC) elements [1–9] or structures [10] and has been found to be a very promising solution.

Shear strengthening of RC beams or bridge girders in old RC structures is one of the most common needs when assessing their strength under the current code requirements (i.e. Eurocodes). This is due to insufficient amount of shear reinforcement, corrosion of existing shear reinforcement, low concrete strength and/or increased design load. Only few researchers [1,11–17] have investigated the use of TRM for shear strengthening of RC beams, the big majority of which were on small or medium-scale rectangular specimens [1,12–17]. A variety of parameters has been studied

* Corresponding author. Tel.: +39 0332 78 5321.
*E-mail address:* Dionysios.Bournas@jrc.ec.europa.eu (D.A. Bournas).

http://dx.doi.org/10.1016/j.compositesb.2016.03.076

including the number of layers [1,11,13,14], the strengthening configuration [12,14], and the performance of TRM versus FRP jackets [1,13,14]. In particular, Azam and Soudki [12] concluded that side-bonded and U-shaped jackets exhibited similar performance in terms of strength. On the contrary, Tetta et al. [14] concluded that U-shaped jackets are much more effective than side-bonded jackets in increasing the shear capacity of beams. Tzoura and Triantafillou [13] on the basis of two specimens retrofitted with U-jackets concluded that TRM jackets are nearly 50% less effective than their counterparts in case of non-anchored jackets, whereas Tetta et al. [14] reported that TRM U-jackets can be as effective as FRP U-jackets.

The problem of end-anchorage of TRM U-jackets in T-beams, so as to delay their early debonding from the concrete substrate, has only been examined in the past by Bruckner et al. [11] and Tzoura and Triantafillou [13]. In both studies a mechanical end-anchorage system (comprising metal sections anchored into the flange by metallic rods) was employed in T-beams strengthened in shear with glass or carbon TRM U-jackets. Despite the fact that the effectiveness of the TRM jackets was significantly improved, an anchorage system with metallic components is susceptible to corrosion and its use is often associated with bearing failures of the composites due to stress concentrations.

From the literature survey it becomes clear that the subject of shear strengthening of RC beams with TRM has not sufficiently been covered. This paper goes several steps beyond the current state-of-the-art as studies shear strengthening of RC T-beams in a systematic way by investigating for the first time in full-scale: (a) the use of a novel end-anchorage system comprising textile-based anchors, which was developed by Koutas et al. (2014) [18] and is used here for the first time in shear strengthening of RC members; (b) the anchorage percentage (50% versus 100%) of the U-jacket; (c) the textile material (carbon versus glass); (d) the textile geometry (8 mm versus 10 mm-mesh opening); and (e) the strengthening system (TRM versus FRP jackets). The number of TRM layers was additionally investigated and a simple design model was proposed to calculate the contribution of anchored TRM jackets to the shear capacity of RC T-beams. Details are provided in the following sections.

## 2. Experimental programme

### 2.1. Test specimens and investigated parameters

The experimental programme included 11 tests performed on full-scale T-beams, simply supported in asymmetric three-point bending. The total length of the T-beams was equal to 6000 mm, whereas the effective flexural span was equal to 3700 mm (Fig. 1a), providing adequate anchorage length to the longitudinal reinforcement. To emulate old detailing practices, the beams were designed to be deficient in shear in one of the two shear spans. To achieve this, the critical shorter shear span of 880 mm length did not include any transverse reinforcement, whereas the larger shear span was over-reinforced including 10-mm diameter stirrups at a spacing of 100 mm.

Strengthening was applied only at the critical shear span aiming to increase its shear resistance. By design, the shear force demand in order to develop the full flexural capacity of the (unretrofitted) beams was targeted to be 3.5 times their shear capacity. To achieve that eight 20 mm-diameter and two 20 mm-diameter deformed bars were placed at the tension and compression zone of the T-beams web, respectively (Fig. 1b). Four 8 mm-diameter deformed bars were additionally placed at the T-beam flanges. The geometrical ratio of tensile steel reinforcement was 3.2%, whereas the effective depth was 385 mm.

The key investigated parameters of this study comprised: (a) the use of textile-based anchors as end-anchorage system of the U-jacket, (b) the number of TRM layers, (c) the textile geometry, (d) the textile material and (e) the comparison between equivalent TRM and FRP jackets. One beam-end was tested as-built and served as the control specimen (CON), whereas the rest ten beams received strengthening. Three different textile meshes were used, namely two carbon textiles (a light-weight and a heavy-weight carbon textile) and a glass textile. Based on the textile material properties (see Section 2.2), seven layers of glass textile are equivalent to one layer of carbon textile and two heavy-weight carbon layers are equivalent to three light-weight carbon layers in terms of the axial stiffness.

Table 1 presents the details of all tested specimens whereas Fig. 2 illustrates all the strengthening configurations adopted. The notation of retrofitted specimens is XN_AP, where X denotes the type of the textile (CL for light carbon, CH for heavy carbon and G for glass) and N denotes the number of layers (2, 3, 4 or 7). AP refers to specimens with anchors with A indicating anchors and P denoting the anchorage percentage of the TRM jackets (50% or 100%). Finally, the suffix R was only used for one specimen received FRP jacketing. The description of the strengthened specimens follows:

- CH2 and CH4: strengthened with 2 and 4 heavy carbon TRM layers, respectively.
- CL3: strengthened with 3 light carbon TRM layers.
- G7: strengthened with 7 glass TRM layers.

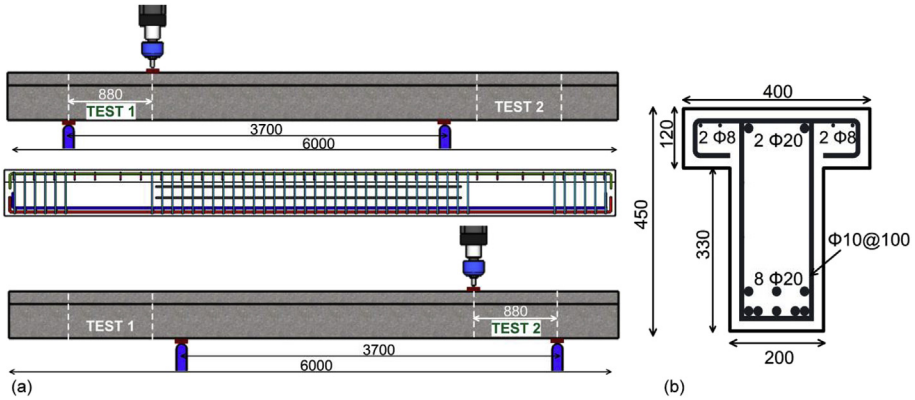


**Fig. 1.** (a) Schematic test set-up; (b) cross-section (dimensions in mm).

**Table 1**
Strengthening configuration and material properties of all specimens.

| Specimen | Textile used[a] | $t$[b] (mm) | $E_f$ (GPa) | No. of layers | $\rho_f$ (‰) | Anchorage percentage (%) | Concrete strength (MPa) | | Mortar strength (MPa) | |
|---|---|---|---|---|---|---|---|---|---|---|
| | | | | | | | Compressive strength | Tensile splitting strength | Compressive strength | Flexural strength |
| CON | – | – | – | – | – | – | 14.0 | 1.39 | – | – |
| CH2 | CH | 0.095 | 225 | 2 | 1.9 | – | 15.2 | 1.67 | 37.4 | 8.79 |
| CL3 | CL | 0.062 | 225 | 3 | 1.9 | – | 13.8 | 1.37 | 35.8 | 8.05 |
| CH4 | CH | 0.095 | 225 | 4 | 3.8 | – | 14.0 | 1.39 | 36.1 | 8.12 |
| G7 | G | 0.044 | 74 | 7 | 3.1 | – | 13.8 | 1.37 | 33.7 | 8.25 |
| CH2_A100 | CH | 0.095 | 225 | 2 | 1.9 | 100 | 15.2 | 1.67 | 34.5 | 8.11 |
| CL3_A100 | CL | 0.062 | 225 | 3 | 1.9 | 100 | 14.9 | 1.60 | 37.9 | 8.74 |
| CH4_A50 | CH | 0.095 | 225 | 4 | 3.8 | 50 | 14.9 | 1.60 | 36.6 | 8.75 |
| CH4_A100 | CH | 0.095 | 225 | 4 | 3.8 | 100 | 14.5 | 1.44 | 33.4 | 8.41 |
| G7_A100 | G | 0.044 | 74 | 7 | 3.1 | 100 | 14.5 | 1.44 | 37.4 | 8.67 |
| CH4_R | CH | 0.095 | 225 | 4 | 3.8 | – | 14.7 | 1.48 | – | – |

[a] CH: Heavy-weight carbon-fibre textile; CL: Light-weight carbon-fibre textile; G: Glass fibre textile.
[b] Nominal thickness of textile in one direction based on the equivalent smeared distribution of fibres.

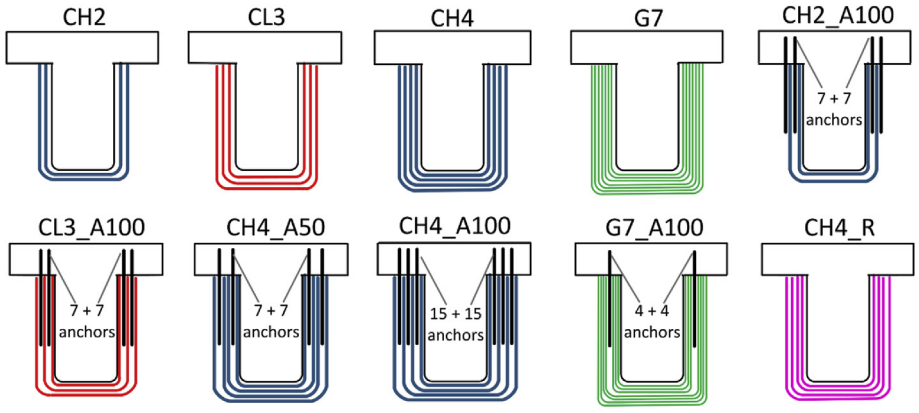


**Fig. 2.** Schematic representation of different strengthening configurations.

- CH2_A100: strengthened with 2 heavy carbon TRM layers anchored by 100% (with seven textile-based anchors on each side of the beam's web).
- CL3_A100: strengthened with 3 light carbon TRM layers anchored by 100% (with seven textile-based anchors per side).
- CH4_A50 and CH4_A100: strengthened with 4 heavy carbon TRM layers anchored by 50% and 100%, respectively (with seven and fifteen anchors per side, respectively).
- G7_A100: strengthened with 7 glass TRM layers anchored by 100% (with four textile-based anchors per side).
- CH4_R: strengthened with 4 carbon FRP layers equivalent to 4 carbon TRM layers.

### 2.2. Materials properties

The specimens were cast in two batches of ready-mix concrete. The compressive and the tensile splitting strength of concrete were obtained experimentally on the day of testing by conducting standard tests on cylinders of 150 mm-diameters and of 300 mm-height. The results are summarized in Table 1 (average values of 3 cylinders) for each specimen. The 20 mm-diameter longitudinal bars used as steel reinforcement had a yield stress, ultimate strength and rupture strain of 571 MPa, 628 MPa and 12%, respectively (experimentally obtained average values from 3 specimens). The 8 mm-diameter longitudinal bar had a yield stress, ultimate strength and rupture strain equal to 568 MPa, 630 MPa and 7.9%, respectively. The corresponding value for the 10 mm-diameter bars used for stirrups were 552 MPa, 593 MPa and 8.4%.

Three different textile reinforcements with equal quantity of fibres in two orthogonal directions were used; two carbon-fibre textiles (a light-weight and a heavy-weight one) and a glass fibre textile. The weight of the light carbon textile reinforcement was 220 g/m$^2$, whereas its nominal thickness (based on the equivalent smeared distribution of fibres) was 0.062 mm (Fig. 3a). According to the manufacturer datasheets, the tensile strength and the modulus of elasticity of the carbon fibres were 4800 MPa and 225 GPa, respectively. The weight of the heavy carbon textile reinforcement was 348 g/m$^2$, whereas its nominal thickness was 0.095 mm (Fig. 3b). The tensile strength and the modulus of elasticity of the carbon fibres were 3800 MPa and 225 GPa, respectively (according to manufacturer datasheets). The heavy carbon textile was also used for the fabrication of all the textile-based anchors. Finally, the glass textile was of 220 g/m$^2$ weight with nominal thickness equal to 0.044 mm (Fig. 3c). The tensile strength and the modulus of elasticity of the glass fibres were 1400 MPa and 74 GPa, respectively (according to the manufacturer datasheets).

As mentioned in the previous section, seven layers of glass fibre textile are equivalent to one layer of carbon-fibre textile in terms of axial stiffness, which is expressed by the product $n_\ell.t.E_f$ [(7*0.044*74)/(1*0.095*225) = 1.07], where $n_\ell$ is the number of TRM layers, $t$ is the nominal thickness of the textile and $E_f$ is the elastic modulus of the fibres. In accordance, two heavy-weight carbon layers are equivalent to three light-weight carbon layers [(2*0.095*225)/(3*0.062*225) = 1.02].

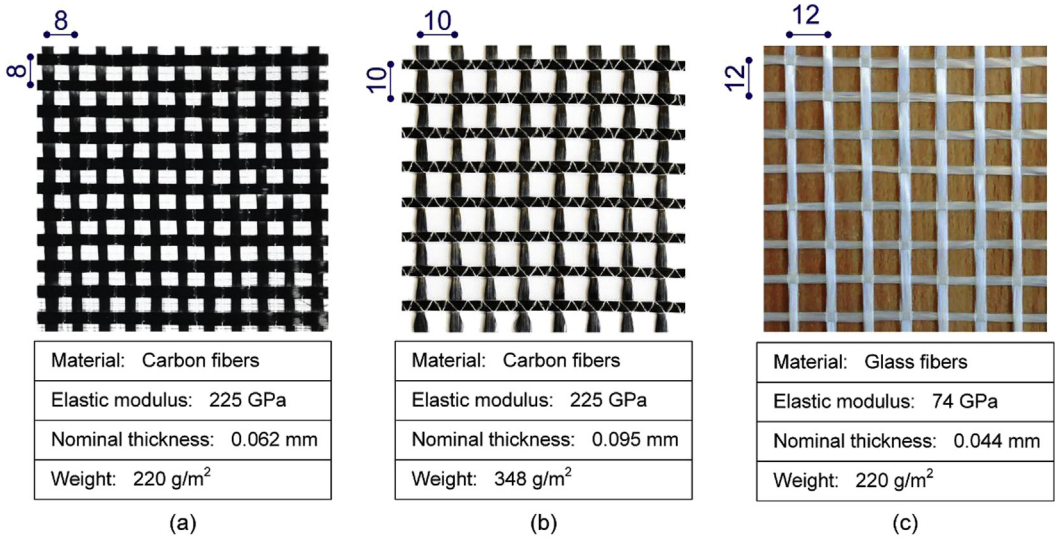


**Fig. 3.** Textiles used in this study: (a) light carbon-fibre textile; (b) heavy carbon-fibre textile; (c) glass fibre textile (dimensions in mm).

For the nine specimens retrofitted with TRM jackets, the binding material used for strengthening was an inorganic dry binder consisting of cement and polymers at a ratio of 8:1 by weight. The water-binder ratio in the mortar was 0.23 : 1 by weight, resulting in plastic consistency and good workability. Table 1 summarizes the strength properties of the mortar (average values of 3 specimens) which were obtained experimentally on the day of testing using prisms of 40 × 40 × 160 mm dimensions, according to the EN 1015-11 [19]. For the FRP retrofitted specimen, the binding material was a commercial epoxy adhesive (two-part epoxy resin with a mixing ratio 4:1 by weight) with an elastic modulus of 3.8 GPa and a tensile strength of 30 MPa (according to the manufacturer datasheets).

### 2.3. Design and fabrication procedure of textile-based anchors

Unlike metallic anchors, textile-based anchors are versatile, non-corrosive, light-weight and compatible with the materials used for TRM jackets. These are the main advantages of the anchorage system proposed in this study, over systems using metallic components. The concept of the textile-based anchors, which were developed and used in Refs. [10,18] for strengthening masonry-infilled RC frames, is the same with that of the spike anchors which are combined with FRP strengthening systems [20–22]. The fan-shaped part of the anchors (see Fig. 4a) serves for the distribution of stresses between the textile reinforcement to be anchored and the anchor itself. The dowel part of the anchor (see Fig. 4a) serves for its installation into holes and anchorage into the concrete mass. All anchors used in this study were identical, and their geometry was based on the following:

1. The length of the anchor's dowel part was selected to be 80 mm (see Fig. 4b). This was the maximum value based on the restrictions imposed by the flange thickness and the position of the compressive steel reinforcement.
2. The length of the anchor's fan was selected to be equal to 200 mm (see Fig. 4b).
3. The fan angle was selected to be 45° (see Fig. 4b) as in the study of Koutas et al. (2014) [18]. Given the fan angle and length, the resulted fan width was 155 mm.
4. Once the fan geometry had been finalized, the amount of anchor fibres in the direction of loading was calculated based on: (a) the maximum number of anchors that could be installed per beam's side, and (b) the maximum area of fibres to be anchored in a U-jacket comprising 4 heavy carbon TRM layers (nearly 300 $mm^2$). By considering that anchors would be installed in 3 sets of 5 in-between the 1st − 2nd, the 2nd − 3rd, and the 3rd − 4th layers (see Section 2.3), the total amount of anchors is equal to 15, which means that the fibres area for each anchor should be 20 $mm^2$ (300 $mm^2$/15).

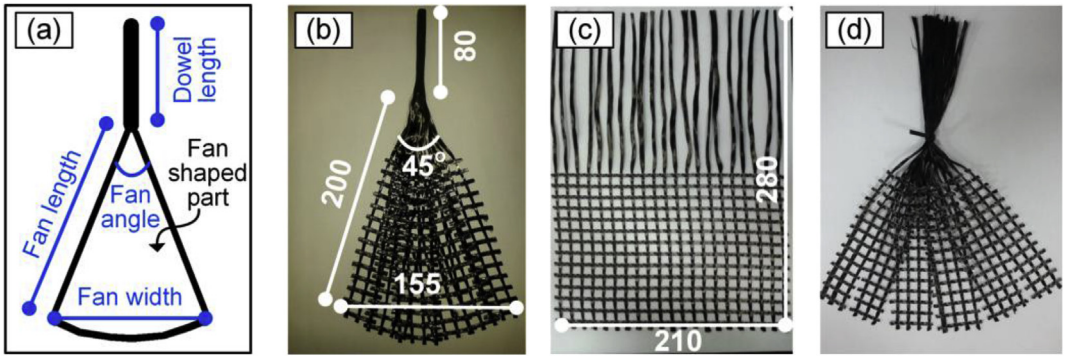


**Fig. 4.** (a) Sketch of textile-based anchor; (b) geometry of the textile-based anchor; (c) partial removal of transverse rovings; (d) separate grid parts of the fanned part of an anchor.

The last row of Table 2 presents the exact percentage of anchorage of the TRM jackets in all specimens with anchors. This is calculated as the ratio of the jacket's axial stiffness (based on the fibres properties) to the axial stiffness of all the anchors in one beam's side (based on the volume of fibres in the dowel part of the anchors).

The procedure followed to form the anchors follows: Initially, a piece of textile was cut in the desired dimensions. The length of the textile was equal to 280 mm while the width was equal to 210 mm (which gives a total fibres area of 20 $mm^2$ in the loading direction). A tow of fibres at one end of the anchor was formed, by removing half of fibre rovings in the direction parallel to the width of the textile (Fig. 4c). For the fanned part of the anchor it was important to be easily applied over a TRM layer and have good bonding conditions. It was therefore necessary to retain the grid of the textile at the fan-shaped part and ensure the alignment of the fibre rovings that would be activated in tension. A way to achieve that was by cutting the fibre rovings in the direction parallel to the width of the textile at certain distances (every two or three vertical rovings), thus creating separate grid parts (Fig. 4d). Finally, both the fibres of the fanned part and the tow were impregnated with epoxy resin followed by a period of 2 days for curing. Impregnation of the fanned part of anchors provides a stable and easy-to-apply material, creating in addition better mechanical interlock conditions between the textile and the mortar. Impregnation of the tow fibres facilitates the insertion of that part of the anchor into the predrilled hole into the slab. A commercial, low viscosity, two-part epoxy resin with tensile strength and modulus of elasticity equal to 72.4 MPa and 3.2 MPa was used to impregnate the fibres of the anchors (the same was used to fill the holes in which the anchors were installed). In order to allow for some flexibility of the anchor during the application process, a small area at the central part was left with dry fibres; these were impregnated locally with epoxy resin during the strengthening application (see Section 2.5).

### 2.4. Tensile capacity of anchors

The tensile capacity of the anchors was experimentally obtained through tensile tests on custom-made bars. The aim was to determine the upper limit of force that the anchors could transfer from the jacket to the concrete mass. For this reason, 3 bars having the same amount of fibres with the anchors (20 $mm^2$ taken from the same carbon textile material used in the anchors), were fabricated and tested according to ACI 440.3R-04 [23] requirements. The tow of fibres used to form the bars had a length of 800 mm and was fully-impregnated with the same epoxy resin used for the impregnation of the anchors tow (see Section 2.3). After curing of the adhesive, the two ends of the bars were inserted into two steel tubes (of 300 mm length each – Fig. 5a) which were filled with the same epoxy resin used to impregnate the anchors fibres. This served for the mounting of the bar-type specimens to testing machine (Fig. 5b).

Uniaxial tensile testing was carried out using a universal testing machine with a load-capacity of 200 kN, at a monotonic loading rate of 5 kN/min. An extensometer was attached on the bar to record its axial deformation during testing (Fig. 5b). The response of the 3 bars tested is given in Fig. 5c in the form of axial stress–strain curves. The average tensile strength and ultimate strain of the 3 bars were 2455 MPa (or 49.1 kN) and 1.85%, respectively.

**Table 2**
Details of specimens with anchored TRM jackets.

| | CH2_A100 | CL3_A100 | CH4_A50 | CH4_A100 | G7_A100 |
|---|---|---|---|---|---|
| Area of anchor fibres, $A_a$ ($mm^2$) | 20 | 20 | 20 | 20 | 20 |
| Number of anchors, $n_a$ | 7 | 7 | 7 | 15 | 4 |
| Modulus of elasticity of anchor fibres, $E_a$ (GPa) | 225 | 225 | 225 | 225 | 225 |
| Area of one TRM layer, $A_\ell$ ($mm^2$) | 74.1 | 48.4 | 74.1 | 74.1 | 34.3 |
| Number of TRM layers, $n_\ell$ | 2 | 3 | 4 | 4 | 7 |
| Modulus of elasticity of TRM layer, $E_f$ (GPa) | 225 | 225 | 225 | 225 | 74 |
| Anchorage Percentage (%) [$(E_a\, n_a\, A_a/E_f\, n_\ell\, A_\ell)$ x 100] | 94.5 | 96.4 | 47.2 | 101.2 | 101.3 |

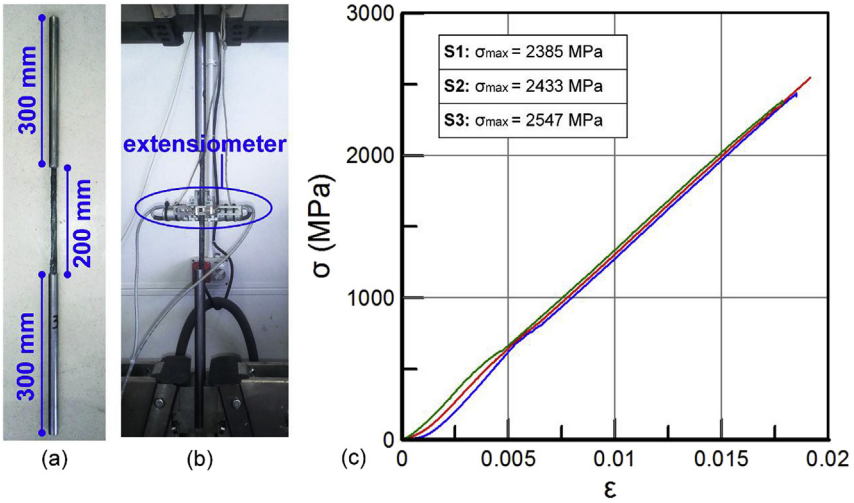


**Fig. 5.** (a) Custom-made carbon-fibre rebar to be used for tensile testing; (b) test set-up for tensile testing of the carbon-fibre rebars; (c) strain versus stress curves for the three tested rebars.

### 2.5. Strengthening procedure

Prior to strengthening a thin layer of concrete cover was removed and a grid of grooves (2–3 mm deep) was created using a grinding machine. The strengthening application in specimens with anchors included the following steps: (1) drilling holes into the T-beam flanges with a diameter of 12 mm and a depth of 80 mm; (2) removing the dust from the holes with compressed air; (3) dampening of the surfaces receiving mortar; (4) application of a mortar layer; (5) bonding the textile by hand pressure (Fig. 6a); (6) application of mortar at the regions that the fanned part of the anchors would cover; (7) filling of the holes with low viscosity epoxy resin (Fig. 6b); (8) local impregnation of the dry fibres of the anchors (those who were not impregnated during anchor preparation) using a two-part epoxy resin with tensile strength and modulus of elasticity equal to 20 MPa and 3 MPa, respectively (Fig. 6c); (9) installation of the anchors, including placement of the anchors into the holes and bonding of the fan over the first textile layer by hand pressure (Fig. 6d); and (10) application of mortar in-between the layers while the previous layer was in a fresh state. In case of specimens strengthened with TRM jackets without anchors, steps (1)–(2) and (7)–(9) were omitted. For the FRP-jacketed specimen the first textile layer was applied on the top of the first resin layer and was then impregnated in-situ with resin using a plastic roll. For additional textile layers the same process was repeated. To avoid stress concentrations in the jacket, the two bottom edges of each beam were rounded to a radius equal to 25 mm.

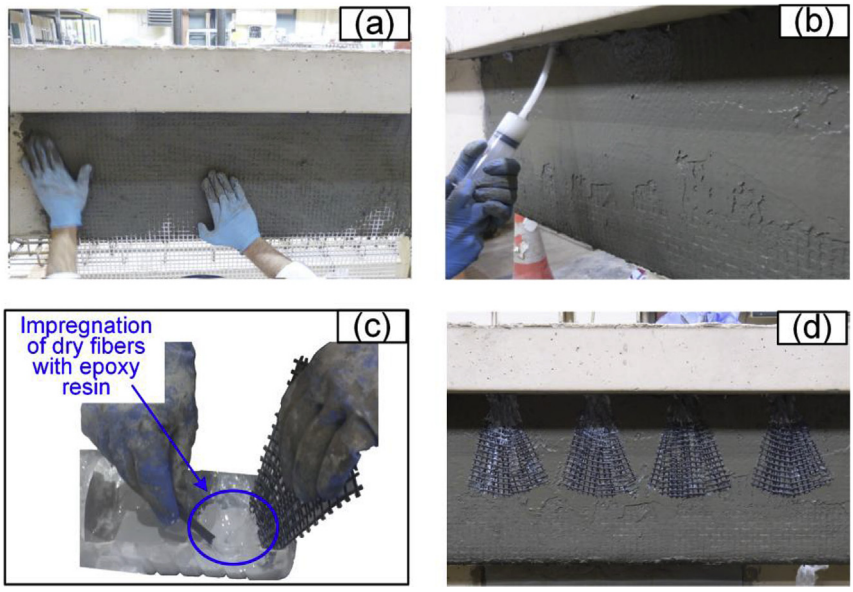


**Fig. 6.** (a) Impregnation of the textile fibres with mortar; (b) injection of epoxy resin into the slab holes; (c) impregnation of dry fibres at the central part of anchor with epoxy resin; (d) textile-based anchors applied over the TRM layer.

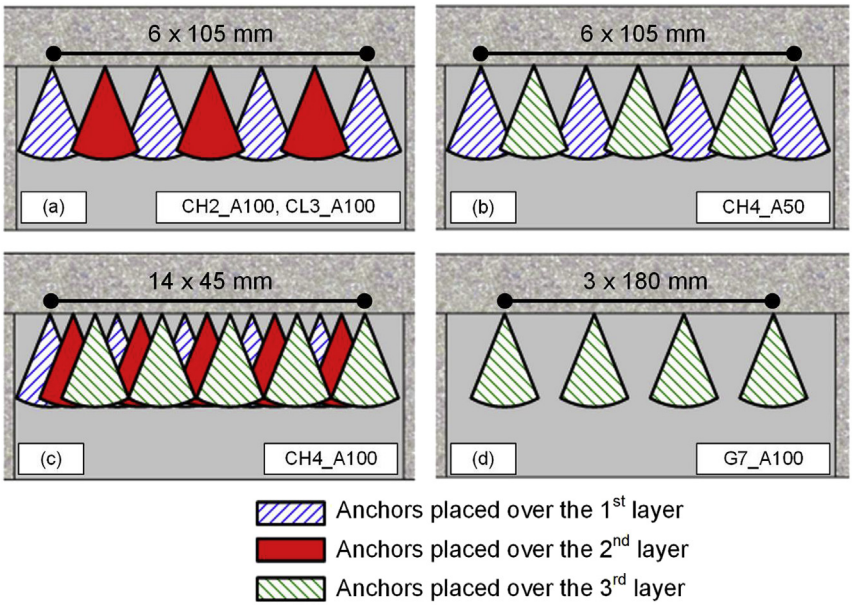


**Fig. 7.** Configuration of anchors in (a) specimens CH2_A100 and CL3_A100; (b) specimen CH4_A50, (c) specimen CH4_A100; (d) specimen G7_A100.

In both CH2_A100 and CL3_A100 specimens, 4 anchors were placed in-between the 1st and the 2nd TRM layer whereas the rest 3 were placed over the 2nd TRM layer (on each side, Fig. 7a). In CH4_A50 specimen, 4 anchors were placed between the 1st and the 2nd TRM layer; whereas the rest 3 were placed in-between the 3rd and the 4th TRM layer (Fig. 7b). In CH4_A100 specimen, 5 anchors were placed in each of the three interfaces between two consecutive TRM layers ($3 \times 5 = 15$, Fig 7c). Finally, in G7_A100 specimen, the 4 anchors were placed between the 3rd and the 4th TRM layer (Fig. 7d).

### 2.6. Experimental setup and procedure

The beams were subjected to monotonic loading using a stiff steel reaction frame and an asymmetric three-point bending set-up configuration (Fig. 8). A vertically positioned, 1000 kN-capacity servo-hydraulic actuator was used for the application of the load at a displacement rate of 0.01 mm/s. As illustrated in Fig. 8, the vertical displacement of the beam was measured at the position of load-application using an external LVDT (Linear Variable Differential Transducer); the displacement measured from this sensor was used to plot the load–displacement response curves of the specimens.

Additionally, the digital image correlation (DIC) technique was employed to monitor relative displacements within the critical shear span, using two high-resolution cameras (on the side of the beam which was free of sensors). In specimens with anchors, strain gauges were attached very close to the end of the TRM jacket (10 mm from the flange) in one side of the beam. The strain gauges were bonded to the face of the TRM jacket at the position of anchors. Finally, strain gauges were mounted to the longitudinal bars at the cross-section of maximum moment to monitor possible yielding of the steel reinforcement. It is noted that all data was synchronized and recorded using a fully-computerized data acquisition system.

## 3. Experimental results

The response of all specimens tested is presented in Fig. 9 in the form of load–displacement curves. Key results are also presented in Table 3. They include: (1) The peak load. (2) The displacement at peak load. (3) The observed failure mode. (4) The shear resistance of the critical shear span, $V_R$, which is the shear force in the critical span at peak load. (5) The contribution of the jacket to the total shear resistance, $V_f$, which is calculated as the shear resistance of the strengthened specimen, $V_{R,str}$, minus the shear resistance of the control specimen, $V_{R,con}$. (6) The shear capacity increase due to strengthening, which is expressed by the ratio, $V_f/V_{R,con}$. (7) The effectiveness of the anchorage system, which is calculated as the ratio of the contribution to shear capacity ($V_f$) of the strengthened specimen with anchors to the contribution of the corresponding specimen without anchors (i.e. CH2_A100 versus CH2 specimen: $112/46 = 2.43$). (8) The effective strain of the jacket, $\varepsilon_{eff}$, which is calculated using Eq. (1) [1]. It is worth mentioning that calculation of $V_f$ values and therefore $\varepsilon_{eff}$ values have been based on the simplified hypothesis that the two mechanisms of carrying forces (concrete contribution and jacket contribution) are superimposed without considering any interaction between them. The interaction between mechanisms of carrying forces is more pronounced when stirrups are used. Thus, other approaches for concrete members strengthened in shear with FRPs, take into account the interaction between the steel and FRP contributions to the shear capacity [24,25].

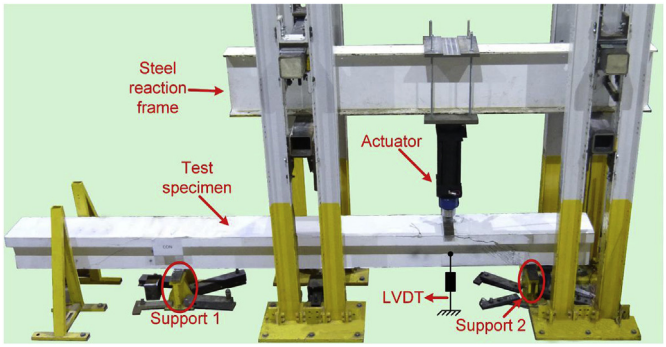


**Fig. 8.** Three-point bending test set-up of T-beams.

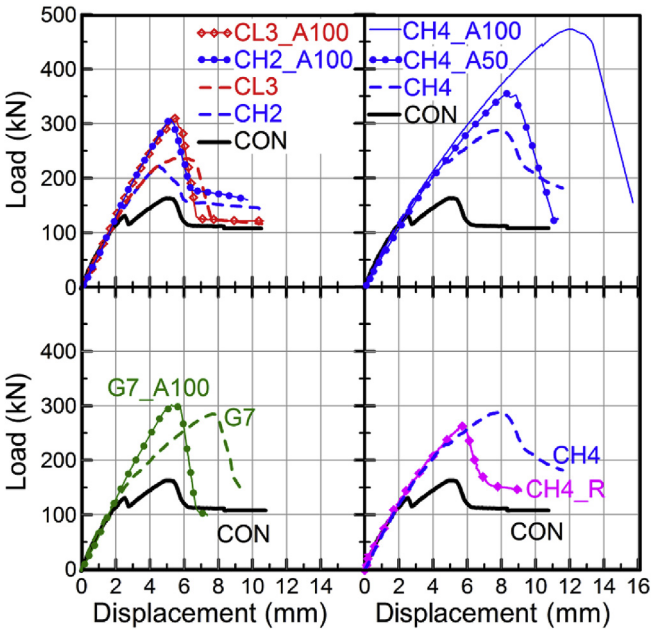


**Fig. 9.** Load versus vertical displacement curves for all tested specimens.

$$\varepsilon_{eff} = V_f \Big/ \left(\rho_f E_f b_w (d - h_s)\right) \quad (1)$$

The control beam (CON) failed in shear at an ultimate load of 163 kN. A large shear crack was firstly formed in the web of the critical shear span (Fig. 10a), which was then propagated into the flange of the T-beam and resulted in significant load drop. All strengthened specimens failed in shear and displayed substantially higher shear resistance (from 37% up to 191%) compared to the control specimen.

### 3.1. Strengthened specimens without anchors

All the strengthened specimens without anchors failed in shear and displayed considerably higher shear resistance (from 37.1 up to 77.4%) compared to the control specimen. In particular, specimen CH2 failed at an ultimate load of 223 kN, resulting in 37.1% increase of the shear capacity. The failure of specimen CH2 (with two layers of heavy carbon textile) was associated with damage on the TRM jacket (Fig. 10b), that included the following local phenomena: (a) slippage of the vertical fibre rovings through the mortar, and (b) partial rupture of the fibres crossing the shear crack. The nature of these local phenomena did not result in very brittle failure mode. In fact, after the peak load was reached, relatively smooth load degradation was recorded.

The peak load attained by specimen CL3 (with three layers of light carbon textile) was 237 kN, which yields 46% increase in the

**Table 3**
Summary of test results.

| Specimen | (1) peak load (kN) | (2) displacement at peak load (mm) | (3) failure mode | (4) $V_R$ (kN) | (5) $V_f$ (kN) | (6) shear capacity increase $V_f/V_{R,con}$ (%) | (7) effectiveness of anchorage system | (8) $\varepsilon_{eff}$ (‰) |
|---|---|---|---|---|---|---|---|---|
| CON | 163 | 5.1 | shear[a] | 124 | – | – | – | – |
| CH2 | 223 | 4.5 | shear[b] | 170 | 46 | 37.1 | – | 2.03 |
| CL3 | 237 | 5.7 | shear[c] | 181 | 57 | 46.0 | – | 2.58 |
| CH4 | 288 | 7.9 | shear[c] | 220 | 95 | 77.4 | – | 2.10 |
| G7 | 285 | 7.7 | shear[c] | 217 | 93 | 75.0 | – | 7.70 |
| CH2_A100 | 309 | 5.3 | shear[d] | 236 | 112 | 90.3 | 2.43 | 4.94 |
| CL3_A100 | 311 | 5.5 | shear[d] | 237 | 113 | 91.1 | 1.98 | 5.11 |
| CH4_A50 | 355 | 8.4 | shear[d] | 271 | 147 | 118.5 | 1.53 | 3.24 |
| CH4_A100 | 473 | 12.0 | shear[e] | 361 | 236 | 191.1 | 2.47 | 5.21 |
| G7_A100 | 302 | 5.3 | shear[f] | 230 | 106 | 85.5 | 1.14 | 8.78 |
| CH4_R | 264 | 5.8 | shear[c] | 201 | 77 | 62.1 | – | 1.70 |

[a] Tensile diagonal cracking.
[b] Slippage of the vertical fibre rovings through the mortar and partial fibres rupture.
[c] Debonding of the jacket.
[d] Rupture of some anchors and pull-out of some other anchors.
[e] Pull-out of anchors due to concrete splitting in the slab.
[f] Fracture of the jacket.

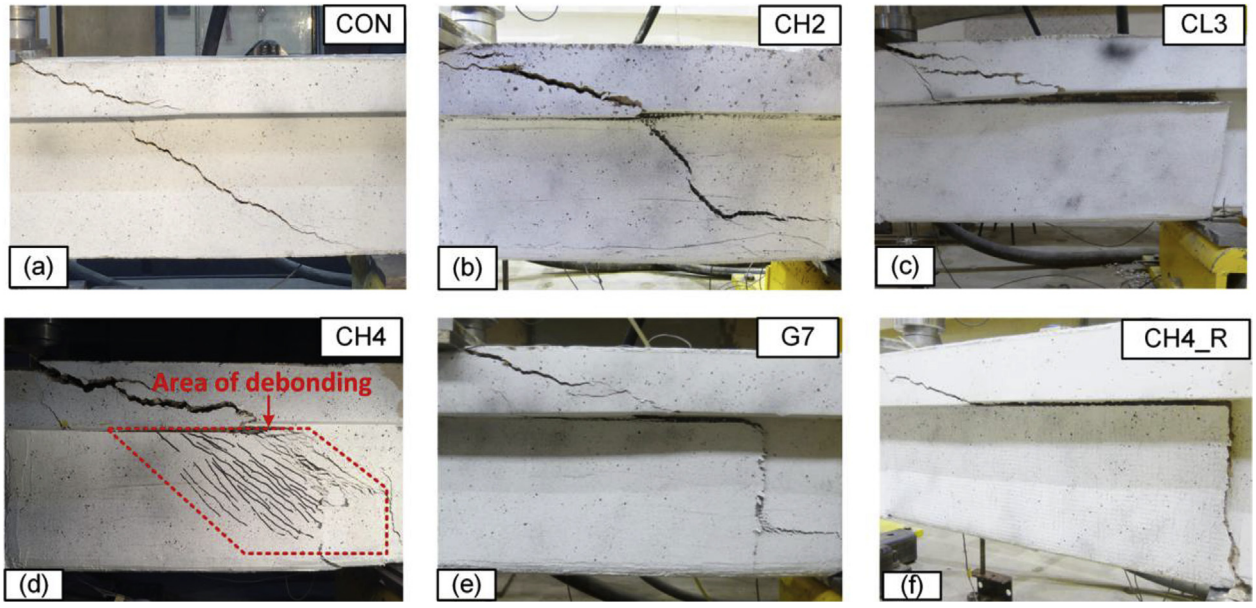


**Fig. 10.** (a) Dominant shear crack in the control beam; (b) local damage of the jacket in specimen CH2; (c)–(e) specimens CL3, CH4 and G7 – debonding of the TRM jacket: peeling off of the concrete cover; (f) debonding of the FRP jacket.

shear capacity. Failure in this specimen was due to debonding of the TRM jacket without including any local damage of the TRM jacket (Fig. 10c). The good bond between the mortar and the concrete substrate resulted in debonding of the TRM jackets from the concrete substrate accompanied with peeling off of the concrete cover.

Specimen CH4 (with four layers of heavy carbon textile) reached a higher load (288 kN) with respect to specimen CH2 (223 kN), owing to the contribution of two extra TRM layers. Its failure was due to debonding of the TRM jacket at a large part (approximately 2/3) of the shear span (Fig. 10d), which was also accompanied by peeling off of the concrete cover. Compared to the control specimen the increase in the shear resistance of specimen CH4 was 77.4%.

Specimen G7 (with seven layers of glass textile) failed in the same way with specimen CH4 (Fig. 10e), reaching an ultimate load of 285 kN that corresponds to 75% increase in the shear capacity.

Finally, specimen CH4_R (with four layers of heavy carbon textile bonded with resin) failed due to debonding of the jacket from the concrete substrate with peeling off of the concrete cover, at an ultimate load equal of 264 kN (62.1% shear capacity increase). Debonding of the FRP jacket was initiated from the point of load-application and propagated instantly to the support (Fig. 10f). Fig. 11 illustrates the part of concrete cover that was bonded to the jacket of CH4 (Fig. 11a) and CH4_R (Fig. 11b) specimen, respectively indicating the very good bond between both adhesives (mortar and resin) with the concrete substrate. The type of failure of specimens CL3, CH4, CH4_R and G7 was rather brittle and always occurred after the shear failure of concrete as shown in Fig. 11 c and d taken after removal of the jacket.

### 3.2. Strengthened specimens with anchors

The debonding of TRM jackets was delayed considerably using textile-based anchors. Specimens CH2_A100 (with two layers of fully anchored heavy carbon textile), CL3_A100 (with three layers of fully anchored light carbon fibre textile), CH4_A50 (with four layers

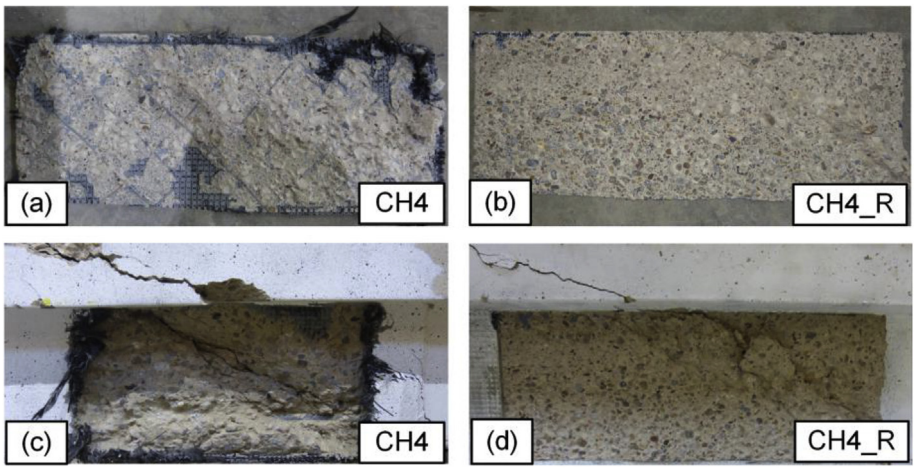


**Fig. 11.** (a)–(b) Part of U-shaped jacket of specimens CH4 and CH4_R; (c)–(d) shear crack in concrete of specimens CH4 and CH4_R after removal of the jacket.

of heavy carbon fibre textile anchored by 50%), CH4_A100 (with four layers of fully anchored heavy carbon fibre textile) and G7_A100 (with seven layers of fully anchored glass fibre textile) failed in shear at even higher loads; 309 kN, 311 kN, 355, 473 and 302 kN, respectively, when compared to the corresponding specimens without anchors; namely CH2, CL3, CH4 and G7.

The shear capacity of specimens CH2_A100, CL3_A100, CH4_A50, CH4_A100 and G7_A100 was increased by 90.3%, 91.1%, 118.5%, 191.1% and 85.5% respectively, with respect to the control specimen. In specimens CH2_A100, CL3_A100 and CH4_A50, debonding of the TRM jacket was initiated at the region where the shear crack on the web intersects with the slab and was expanded to a broader area of the beam when the anchors failed due to fibres rupture or pull-out from the slab (Fig. 12a, b and c). In particular, in specimen CH2_A100, 5 (out of 14) anchors were pulled out from the slab, while 3 anchors (out of 14) were ruptured. In specimens CL3_A100 and CH4_A50, 4 anchors (out of 14) were ruptured, whereas 4 anchors (out of 14) were pulled out from the slab. Failure of specimen CH4_A100 was attributed to anchors pull-out (8 on each side) due to concrete splitting at the two flanges (Fig. 12d). Finally, failure of specimen G7_A100 was attributed to fracture of the glass TRM jacket (Fig. 12e) without including any failure of the anchors.

Strain gauges were affixed at the positions of anchors in order to better understand the response of the specimens with anchors. Fig. 13 illustrates the load versus TRM jacket strains in specimen CH4_A50, at the positions of anchors (see Section 2.6). As shown in Fig. 13, the anchors activation started with a phase difference from the load-application position towards the support. The TRM jacket at the vicinity of anchor '3', debonded before the peak load, namely at around 265 kN. Strain gauge '4' started recording strains with higher rate between 300 kN and 335 kN when debonding of TRM

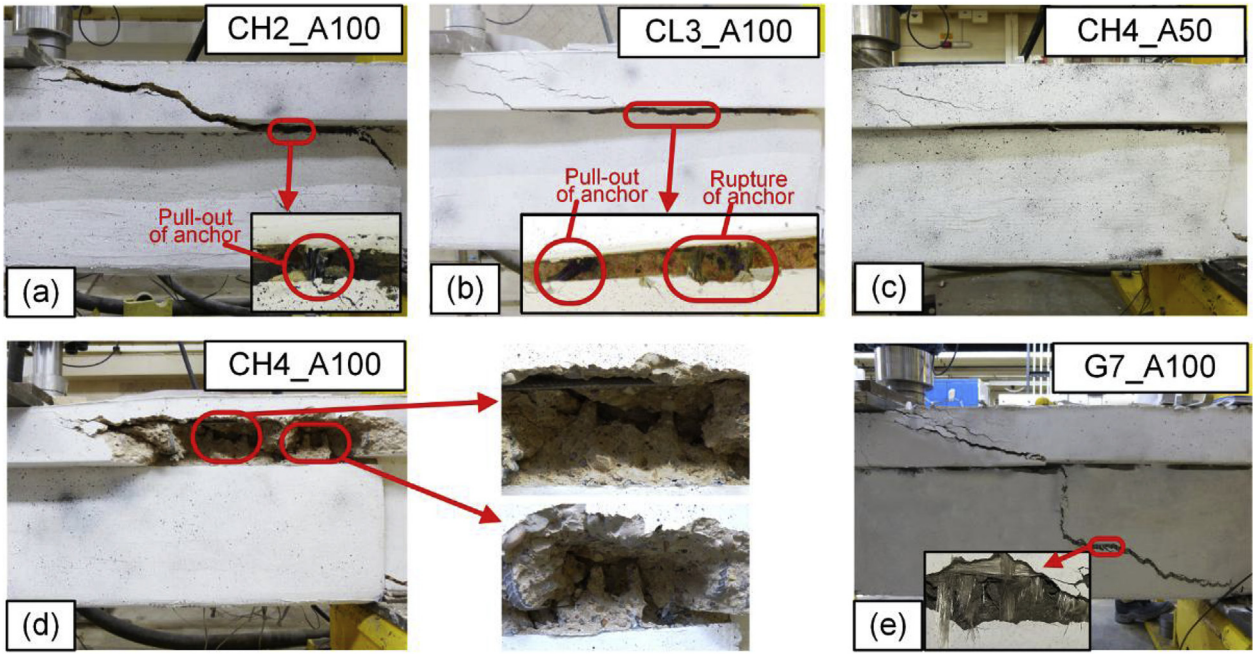


**Fig. 12.** Failure modes of TRM-retrofitted specimens with anchors: (a)–(c) Specimens CH2_A100, CL3_A100 and CH4_A50 – rupture of some anchors and pull-out of the rest; (d) failure of specimen CH4_A100 due to concrete splitting in the slab; (f) fracture of glass TRM jacket in specimen G7_A100.

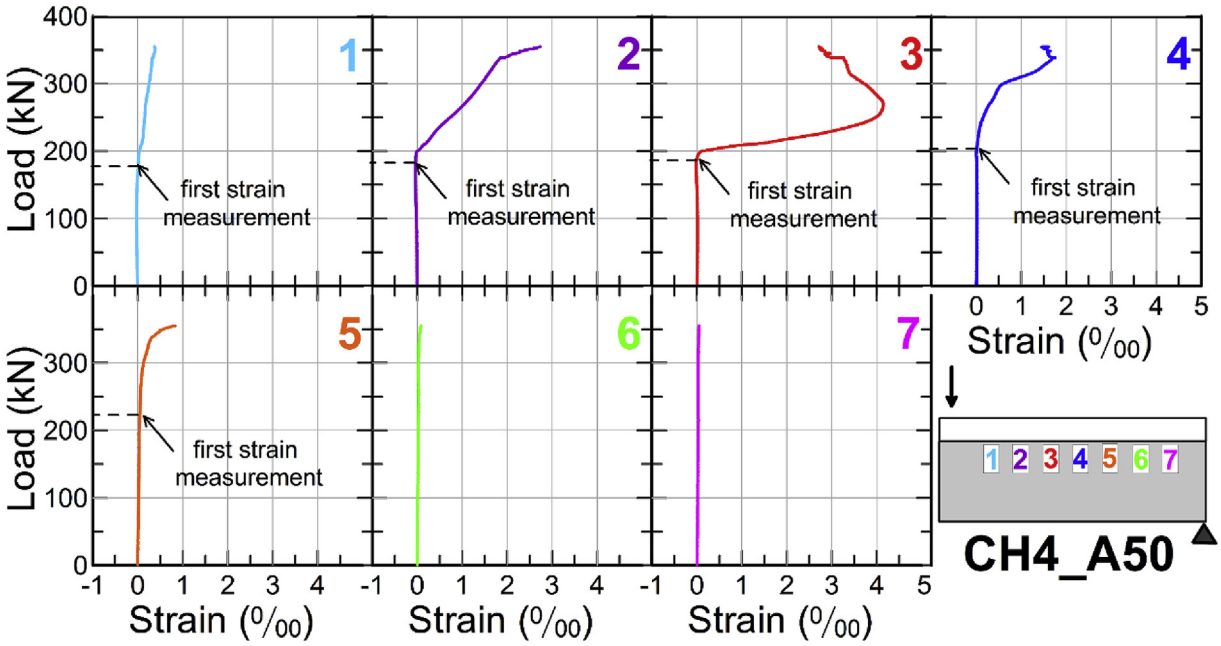


**Fig. 13.** Strain versus load curves using strain gauges readings in specimen CH4_A50.

jacket propagated progressively to the vicinity of anchor '4'. At that point (335 kN), strains of anchors '2' and '5' are increasing in higher rate. This rate change in development of strains is probably related to the redistribution of stresses from one anchor to another one. The behaviour observed to all strengthened specimens with anchors was identical.

## 4. Discussion

### 4.1. Effect of investigated parameters

All specimens responded as designed and failed in shear prior to yielding of the longitudinal steel reinforcement. This response allowed for the evaluation of the capacity of all strengthening systems in increasing the shear resistance of the full-scale T-beams. In terms of the various parameters investigated in this experimental programme, an examination of the results (Table 3) in terms of shear capacity, failure modes and effective strains, revealed the following information.

#### 4.1.1. Anchorage system of the U-jacket

The effectiveness of the anchored U-jackets in increasing the shear capacity of the T-beam (specimens CH2_A100; CL3_A100; CH4_A50; CH4_A100; G7_A100) was from 1.14 to 2.47 times the effectiveness of the non-anchored jackets (see Table 3). The increase was depending on the number of the TRM layers, the percentage of jacket's anchorage, and the material of the fibres in the jacket.

Particularly, in specimen CH2_A100, the use of 7 anchors per side of the beam (that provided full anchorage of the applied layers) increased the shear resistance of the beam by 90.3% compared to the control specimen, whereas the effectiveness of the TRM jacket was increased by 143% compared to the corresponding specimen without anchors (CH2). The full anchorage of three light carbon layers provided by 7 anchors per beam's side (CL3_A100) improved the effectiveness of the TRM jacket by 98% compared with its counterpart specimen without anchors (CL3) resulting in 91.1% increase in the shear resistance compared with the control specimen. The 50% (CH4_A50) and 100% (CH4_A100) anchorage of four heavy carbon layers increased the shear resistance of the control specimen dramatically, namely by 118.5% and 191.1%, respectively, improving at the same time the effectiveness of the TRM jacket by 53% and 147%, respectively, when compared to specimen CH4. In specimen G7_A100, the effectiveness of glass TRM jacket was improved by only 14% using 4 anchors on each side of the beam, whereas its shear resistance increased by 85.5% as compared to the control specimen. In this case the limited effectiveness of the anchorage system is attributed to the fact that the non-anchored jacket had already developed an effective strain (7.70‰) that was just 12% lower than the effective strain developed at fibres rupture in the anchored jacket (8.78‰).

In specimens CH2_A100, CL3_A100 and CH4_A50, the TRM jacket debonded following the failure of the anchorage system. The local damage of the TRM jacket which occurred in specimen CH2 without anchors (including slippage of the vertical fibre rovings through the mortar and partial fibres rupture) was limited when the jacket was anchored in specimen CH2_A100, thanks to the additional fibres provided by the fan-part of the anchors (Figs. 6d and 7). It is important to note that specimen CH2_A100, strengthened with two carbon TRM layers and anchors, was 17% more effective (in terms of $V_f$, see in Table 3) than specimen CH4 which was strengthened with four carbon and had approximately 28% more material. This can lead to significant cost benefits in real applications due to the considerable material savings. In specimen CH4_A100, the anchors were pulled out suddenly from the slab due to concrete splitting before reaching their tensile capacity. Finally, failure of specimen G7_A100 was due to fracture of the glass TRM jacket without any failure of the anchorage system.

The beam strengthened with two and four heavy carbon (CH2 and CH4) TRM layers and three light carbon (CL3) TRM layers without anchors had effective strain, $\varepsilon_{eff}$, equal to 2.03‰, 2.10‰ and 2.58‰, respectively (see Table 3). The effectiveness of carbon TRM jacket was considerably improved by providing full anchorage to the TRM jackets with textile-based anchors. In particular, the TRM jacket effective strain, $\varepsilon_{eff}$ of specimens CH2_A100, CH4_A100 and CL3_A100 was equal to 4.94‰, 5.21‰, and 5.11‰, respectively. The corresponding value for CH4_A50 specimen was 3.24‰.

Unexpectedly, specimen CH4_A100 failed in shear due to concrete splitting in the flange of the T-beams (Fig. 12d). Such a failure mode, which is related to the tensile strength of the concrete, sets an upper limit on the shear capacity increase of the U-TRM jackets anchored in the slab. In fact, by multiplying the experimentally observed splitting area [$2^*(\ell_v + \ell_h)^*0.6^*L_s$ as shown in Fig. 14] by the concrete tensile splitting strength ($f_{ct}$ = 1.44 MPa for specimen CH4_A100), the resulted value is 243 kN, which is in very good agreement with the actual contribution of the anchored jacket to the shear capacity of the beam (236 kN).

#### 4.1.2. Number of layers

The contribution of TRM jackets to the beam shear capacity was increased in an almost proportional way with the number of TRM layers (for the same type of textile). Doubling the amount of reinforcement of the non-anchored jackets (4 layers instead of 2) resulted in 2.09 times increase of the contribution to the shear resistance (CH4 versus CH2). The corresponding increase was 2.12 when anchors were used to provide full anchorage of the TRM jacket (CH4_A100 versus CH2_A100).

As described in Section 3, a change in the failure mode was witnessed when the number of layers was increased from two to four in case of specimens without anchors. In particular, the failure of specimen received two layers (CH2) was dominated by local damage of the TRM jacket (the vertical fibre rovings crossing the developed shear crack at the jacket experienced a combination of slippage through the mortar and partial rupture). Contrary, the failure mode of specimen received four layers (CH4) is associated to the failure of the concrete substrate with no damage in the composite jacket. Thus, the increase in the number of layers prevented these local phenomena and as a result the damage was shifted to the concrete substrate. This is attributed to the better mechanical interlock conditions created by the overlapping of multiple textile layers as also reported in Ref. [14].

The effective strains of specimens received 2 and 4 non-anchored TRM layers (CH2, CH4) were 2.03‰ and 2.10‰, respectively. The corresponding values for specimens received 2 and 4 fully anchored TRM layers (CH2_A100 and CH4_A100) were 4.94‰ and 5.21‰, respectively.

#### 4.1.3. Textile geometry

Specimens CH2 and CL3 received correspondingly 2 and 3 layers carbon textile of different geometry, having although the same external reinforcement ratio ($\rho_f$ = 1.9‰). The light carbon textile used in specimen CL3 has denser mesh-pattern and TEX (which is the weight of each roving in g/km) equal to 880; whereas the TEX of the heavy carbon textile is equal to 1740. The shear capacity increase of CH2 and CL3 specimens was 37.1% and 46.0%, respectively (compared to the control specimen), whereas the effective strains at ultimate load were 2.03‰ and 2.58‰, respectively.

A comparison of the results for specimens CH2 and CL3 shows that the textile geometry has an effect on the failure mode. As mentioned before, CH2 specimen failed due to local damage of the TRM jacket (slippage of fibres through the mortar and partial rupture of fibres crossing the shear crack) in contrary to specimen CL3 that failed due to debonding of the TRM jacket from the concrete substrate. The difference in failure mode observed in these specimens is possibly associated with the dense mesh-pattern of the textile (thanks to the smaller mesh size of the light-weight carbon-fibre textile) in specimen CL3, which resulted in better fibres distribution along the shear span and therefore the mechanical interlock between the textile and the mortar was improved.

The shear capacity increase of the corresponding specimens with full anchored TRM jacket (CH2_A100, CL3_A100) was 90.3% and 91.1%, respectively (compared to the control specimen), whereas the effective strains were 4.94‰ and 5.11‰, respectively. Thus, the presence of anchors mitigated the effect of textile geometry in specimens CH2_A100 and CL3_A100, as the failure of these specimens was governed by the behaviour of anchors (rupture of some anchors and pull-out of some other anchors) and not from the behaviour of TRM jacket as in case of the non-anchored specimens (CH2, CL3).

#### 4.1.4. Textile material

Specimen G7 strengthened with seven glass textile layers had approximately the same shear capacity with specimen CH4 that received four heavy carbon textile layers, despite the fact that seven glass textile layers are equivalent to just one heavy carbon textile layer (in terms of axial stiffness as explained in Section 2.2). In specific, the shear capacity increase of specimens G7 and CH4 was 77.4% and 75.0%, respectively. As a result, the effective strain of the TRM jacket, $\varepsilon_{eff}$, was much higher in specimen G7 (7.70‰) when compared with that of CH4 (2.10‰). The latter indicates that glass fibres are more effective than carbon fibres in shear strengthening of concrete beams with U-shaped TRM jackets. Both specimens exhibited similar failure mode, namely debonding of the TRM jacket from the concrete substrate.

The evaluation of the effect of textile material in case of anchored TRM jacketing is not feasible, as the failure of specimen CH4_A100 was due to concrete splitting in a part of the slab, whereas the failure of specimen G7_A100 was due to fracture of the glass TRM jacket.

#### 4.1.5. Adhesive material (TRM vs. FRP jackets)

The effect of the adhesive material on the shear capacity increase of non-anchored U-jackets was negligible. When resin was used as bonding agent (specimen CH4_R with four heavy carbon

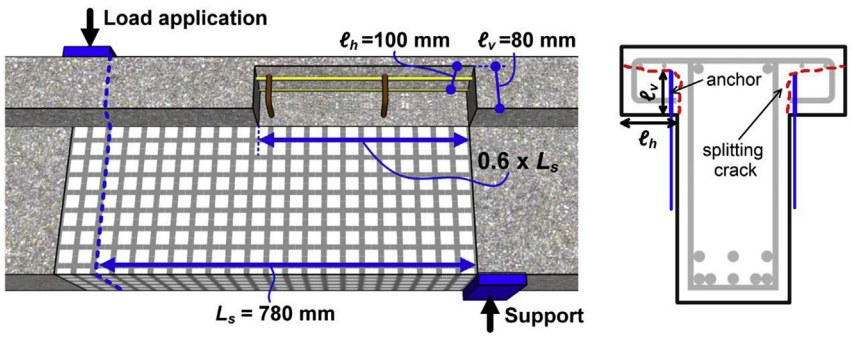


**Fig. 14.** Concrete splitting area and length of splitting crack developed in specimen CH4_A100.

textile layers) the shear capacity of the beam was increased by 62.1%. This is marginally less than the capacity increase observed in its mortar impregnated counterpart specimen CH4 (77.4%). The effective strains of specimens CH4 and CH4_R were 2.10‰ and 1.70‰, respectively. The failure mode in both specimens was associated with debonding of the jacket; the strong bond between the adhesive material (mortar or resin) with the substrate concrete resulted in peeling off of the concrete substrate. It is noted, that the corner radius at the bottom edges of the beam's web (equal to 25 mm for both TRM and FRP systems) did not have any effect on the failure mode of the beams.

### 4.2. Deformation aspects of jackets based on DIC

Images of the in-plane and out-of-plane deformations of the TRM jackets, obtained using DIC measurements at the instant of maximum load, are presented in Fig. 15 for each retrofitted specimen (one side of the jacket was monitored). In specimens with anchored jackets, white and black dots are used at the top of TRM jacket to indicate which anchors were (white dots) and which not (black dots) activated based on the strain gauges readings.

Application of anchors reduced the evolution of the jacket debonding (out-of-plane deformations) at the shear span of the beam. The TRM jacket of specimen CH2 started debonding but local damage of the jacket finally dominated the failure. In specimen CH2_A100, although these local phenomena were limited compared to CH2, signs of local damage of the jacket (two cracks were formed) were evident in-between the anchors. Debonding of the TRM jacket in specimen CL3_A100 was significantly reduced (in both amplitude and width) than the corresponding specimen without anchors (CL3). In specimen CH4_A50, the use of anchors that provided 50% anchorage of the applied TRM layers substantially limited the extent of TRM jacket debonding as compared to its counterpart specimen without anchors (CH4). The performance of specimen CH4_A100 was quite impressive as the TRM jacket debonding was prevented up to a load of 473 kN that the anchors failed. The presence of anchors in specimen G7_A100 slightly reduced the TRM debonding as compared to specimen G7, as the glass TRM jacket fractured before the full activation of the applied anchors.

## 5. Design model

### 5.1. Methodology

In this paragraph, a simplifying methodology for calculating the contribution of anchored TRM U-jackets to the shear resistance of RC beams is proposed. It is based on the following assumptions:

- The number of anchors provided is sufficient to increase the effectiveness of the non-anchored jacket. In lack of data, this could be translated as a minimum number of anchors which corresponds to anchorage of 50% of the jacket fibres.
- The anchored TRM jacket is idealized as discrete vertical shear links at a distance $s$ (distance between the anchors) which connect the compression zone with the tensile (longitudinal) reinforcement of the beam. The shear links have the properties of the anchors. By this idealization the behaviour of the jacket is governed by the behaviour of the anchors, and the contribution of each (U-jacket and anchors) is not considered separately.

By applying the Morsch truss analogy, the following equation can be used to calculate the contribution of anchored TRM U-jackets to the total shear resistance of a T-beam:

$$V_f = A_{anc} f_{fe,anc} \frac{h_w}{s} \cot\theta \tag{2}$$

Similarly to the case of internal steel stirrups, the term $(h_w/s)$ $\cot\theta$ in Eq. (2) determines the number of anchors that are activated in tension.

The effective strength of the anchors, $f_{fe,anc}$, is a reduced value of their tensile capacity, $f_{f,anc}$, to account for: (a) local concentration of stresses at the point where the anchor enters the concrete slab, and (b) the non-uniform distribution of stresses between activated anchors. It is expressed by the following equation:

$$f_{fe,anc} = \eta_e f_{f,anc} \tag{3}$$

where $\eta_e$ is the strength reduction factor with values less than 1.0.

It is important to note that there are two upper limits for the value of $V_f$ calculated according to Eq. (2): (a) the shear force corresponding to rupture of the fibres in the TRM jacket (as in the case of specimen G7_A100), and (b) the force at which the concrete of the slab fails due to tensile splitting (as in the case of specimen CH4_A100).

### 5.2. Model calibration to the test results

Using the experimental values of $V_f$ (calculated according to the approach that the concrete and jacket contribution are superimposed without considering any interaction between; see Table 4), the effective strength of the anchors, $f_{fe,anc}$, was calculated using Eq. (2) for specimens CH2_A100, CL3_A100 and CH4_A50, in which the ultimate load was governed by the anchors failure (rupture or pull-out from the slab). The results are presented in Table 4 (using $\theta = 45^o$).

The effective strength of the anchors was almost the same for the two cases with 100% anchorage of the fibres of the jacket, and approximately equal to 900 MPa. This value gives a strength reduction factor of 0.37 when divided by the tensile capacity reported in Section 2.4 (2455 MPa). In the case of 50% anchorage of the jacket's fibres, the resulting value was higher and equal to 1185 MPa, which yields a strength reduction factor of 0.48.

Although it seems that anchoring 50% of the jacket fibres results in higher effective strength of the anchors, it is not safe to conclude due to the limited available data. For this reason, and before more experimental data will be available, a value of $\eta_e = 0.3$ is suggested for design purposes.

## 6. Conclusions

This paper presents a large experimental investigation on the effectiveness of TRM U-jackets in shear strengthening of full-scale RC T-beams. Key parameters of this study were: (a) the use of textile-based anchors as end-anchorage system of the U-jacket, (b) the number of TRM layers, (c) the textile geometry, (d) the textile material (two carbon-fibre textiles and a glass fibre textile) and (e) the performance of equivalent FRP jackets for the case without anchors. For this purpose, eleven shear-deficient T-beams were subjected to three-point bending under monotonic loading: one was tested as-built, whereas the rest ten were strengthened prior to testing. The main conclusions drawn from this study are summarized as follows:

- The use of textile-based anchors dramatically increases the effectiveness of carbon TRM U-jackets. Full anchorage of the carbon TRM layers improved the effectiveness of the jackets by

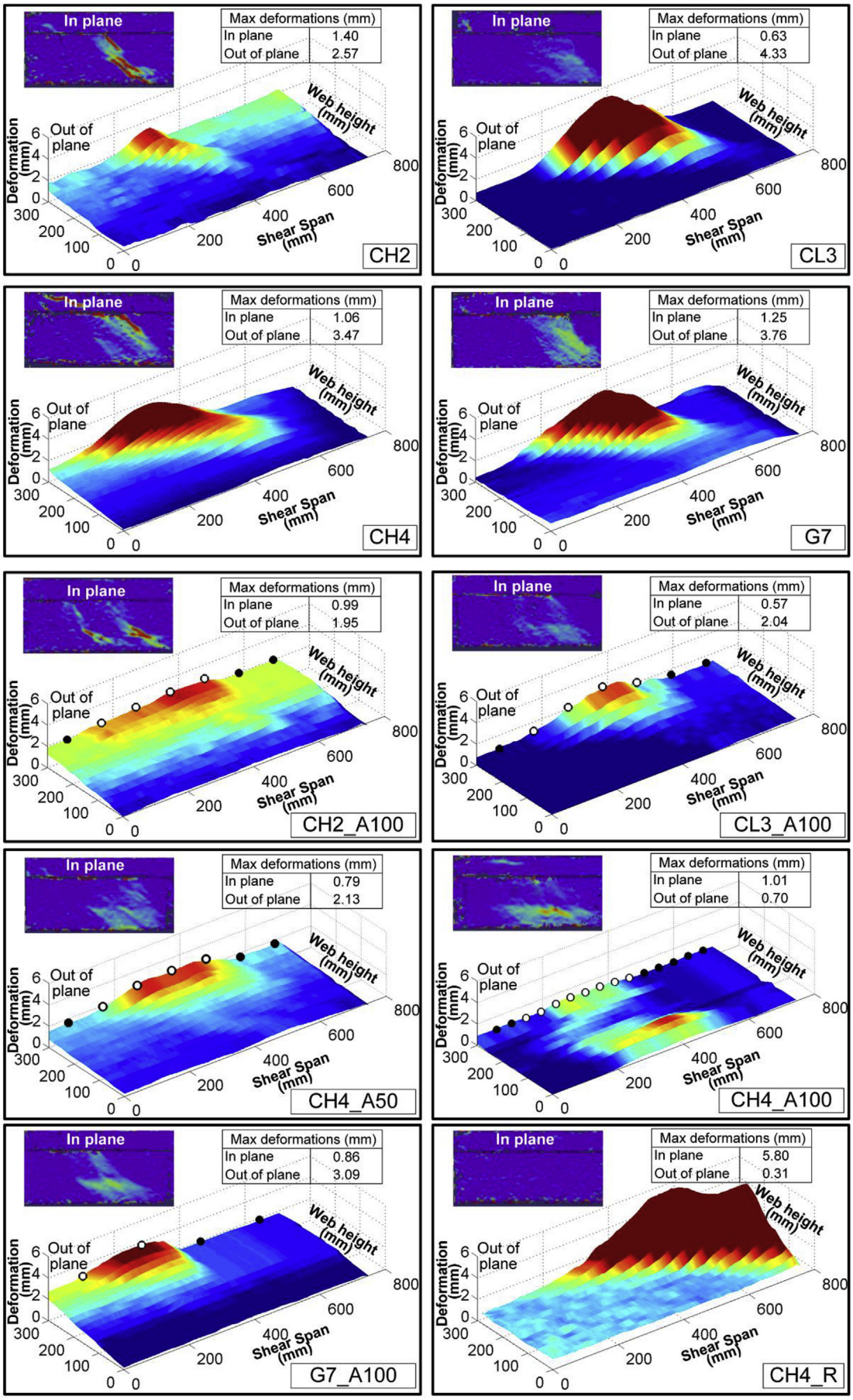


**Fig. 15.** Field of vertical axis (in-plane) and out-of-plane (indicating debonding) deformations in the critical shear span of the strengthened specimens at the instant of peak load.

**Table 4**
Effective strength of anchors and strength reduction factor for specimens failed due to anchorage loss.

| Specimen | $V_{f,exp}$ (kN) | $A_{anc}$ (mm$^2$) | $h_w/s$ | $f_{fe,anc}$ (MPa) | $\eta_e$ |
|---|---|---|---|---|---|
| CH2_A100 | 112 | 40[a] | 3.1 | 903 | 0.37 |
| CL3_A100 | 113 | 40 | 3.1 | 911 | 0.37 |
| CH4_A50 | 147 | 40 | 3.1 | 1185 | 0.48 |

[a] Fibres area of two anchors (one per each beam's side).

98%–148%, depending on the number of TRM layers and the textile geometry.

- High effective strains, $\varepsilon_{eff}$ can be achieved when the TRM jacket is anchored. Values ranging from 3.24‰ to 5.21‰ (depending on the number of TRM layers and the amount of anchors) were achieved in this study. Contrary, the effective strain in the TRM jackets without anchors ranged between 2.03‰ and 2.58‰.
- Anchoring the 2 (heavy) carbon layers TRM jacket is almost equivalent to the application of 4 (heavy) carbon TRM layers without anchorage, yielding significant cost benefits.
- The number of layers affects the failure mode of non-anchored TRM U-jackets. When number of layers increases, local damage of the TRM jacket (partial fibres rupture and slippage of fibre filaments through the mortar) is prevented and damage is shifted to the concrete substrate.
- In non-anchored jackets, different textile geometries with the same reinforcement ratio result in practically the same load increase but different failure modes develop. In anchored jackets the effect of the different textile geometry is eliminated as the failure is governed by the anchors behaviour.
- The effect of different textile material (glass versus carbon) is more pronounced in non-anchored jackets, where seven glass textile layers had approximately the same shear capacity with four heavy carbon textile layers, despite the fact that seven glass textile layers were equivalent to just one heavy carbon textile layer (in terms of axial stiffness).
- TRM U-jackets are as effective as FRP U-jackets in increasing the shear capacity of full-scale RC T-beams.
- A simple analytical model which calculates the contribution of anchored TRM jackets to the shear capacity of RC T-beams can be used for design purposes.

The above conclusions should be treated carefully as they are based on limited number of specimens. In this respect, future research should be directed towards providing a better understanding of parameters including jackets reinforcement ratio, shear span of beams, anchors geometry and embedment length, allowing for more reliable calculation of the strength reduction factor $n_e$ introduced in this study. Finally, it should be noted that the use of resin to fix the anchors into the slab could reduce their anchorage capacity, and for this reason future research should be directed on assessing the performance of anchored TRM jackets under high temperatures.

## Acknowledgements

The authors wish to thank the lab managers Tom Buss and Mike Langford, the chief technician Nigel Rook, the technicians Balbir Loyla, Gary Davies, Sam Cook and Luke Bedford and the PhD candidate Saad Raoof for their assistance in the experimental work. The research described in this paper has been co-financed by the UK Engineering and Physical Sciences Research Council (EP/L50502X/1) and the University of Nottingham through the Dean of Engineering Prize, a scheme for pump priming support for early career academic staff.

## Notation

| | |
|---|---|
| $A_a$ | Area of anchor fibres |
| $A_{anc}$ | Area of two anchors (one anchor per beam's side) |
| $A_\ell$ | Area of one TRM layer |
| $E_a$ | Modulus of elasticity of anchor fibres |
| $E_f$ | Modulus of elasticity of the fibres |
| $L_s$ | Clear shear span |
| $V_f$ | Contribution of strengthening to the shear capacity of the beam |
| $b_w$ | Width of the beam |
| $d$ | Effective depth of the section |
| $f_{ct}$ | Tensile splitting of concrete |
| $f_{f,anc}$ | Tensile capacity of anchor |
| $f_{fe,anc}$ | Effective strength of anchors |
| $h_s$ | Depth of the slab |
| $h_w$ | Height of T-beam's web |
| $\ell_h$ | Beam's flange width |
| $\ell_v$ | Depth of the anchorage |
| $n_a$ | Number of anchors |
| $n_\ell$ | Number of TRM layers |
| $s$ | Anchors spacing |
| $t$ | Nominal thickness of the textile |
| $\varepsilon_{eff}$ | Effective strain |
| $\eta_e$ | Strength reduction factor |
| $\theta$ | Angle between the shear crack and the axis of the beam |
| $\rho_f$ | Geometrical reinforcement ratio of the composite material |

## References

[1] Triantafillou TC, Papanicolaou CG. Shear strengthening of reinforced concrete members with textile reinforced mortar (TRM) jackets. Mater Struct 2006;39(1):93–103.
[2] Bournas DA, Lontou PV, Papanicolaou CG, Triantafillou TC. Textile-reinforced mortar versus fiber-reinforced polymer confinement in reinforced concrete columns. ACI Struct J 2007;104(6).
[3] Bournas DA, Triantafillou TC, Zygouris K, Stavropoulos F. Textile-reinforced mortar versus FRP jacketing in seismic retrofitting of RC columns with continuous or Lap-spliced deformed bars. J Comp Constr 2009;13(5):360–71.
[4] Bournas DA, Triantafillou TC. Bond strength of lap-spliced bars in concrete confined with composite jackets. J Comp Constr 2011;15(2):156–67.
[5] Bournas DA, Triantafillou TC. Bar buckling in RC columns confined with composite materials. J Comp Constr 2011;15(3):393–403.
[6] Jesse F, Weiland S, Curbach M. Flexural strengthening of RC structures with textile-reinforced concrete. Am Concr Inst 2008:49–58. Special Publication 250.
[7] Elsanadedy HM, Almusallam TH, Alsayed SH, Al-Salloum YA. Flexural strengthening of RC beams using textile reinforced mortar–experimental and numerical study. J Comp Struct 2013;97:40–5.
[8] Al-Salloum YA, Siddiqui NA, Elsanadedy HM, Abadel AA, Aqel MA. Textile-reinforced mortar versus FRP as strengthening material for seismically deficient RC beam-column joints. J Comp Constr 2011;15(6):920–33.
[9] Koutas LN, Bournas DA. Flexural strengthening of two-way RC slabs with textile-reinforced mortar: experimental investigation and design equations. J Compos Constr 2016. http://dx.doi.org/10.1061/(ASCE)CC.1943-5614.0000713 [Epub ahead of print].
[10] Koutas L, Bousias SN, Triantafillou TC. Seismic strengthening of masonry-infilled RC frames with TRM: experimental study. J Comp Constr 2015;19(2):04014048. http://dx.doi.org/10.1061/(ASCE)CC.1943-5614.0000507.
[11] Brückner A, Ortlepp R, Curbach M. Anchoring of shear strengthening for T-beams made of textile reinforced concrete (TRC). Mater Struct 2008;41(2):407–18.
[12] Azam R, Soudki K. FRCM strengthening of shear-critical RC beams. J Comp Constr 2014;18(5):04014012. http://dx.doi.org/10.1061/(ASCE)CC.1943-5614.0000464.
[13] Tzoura E, Triantafillou TC. Shear strengthening of reinforced concrete T-beams under cyclic loading with TRM or FRP jackets. Mater Struct 2016;49(1):17–28. http://dx.doi.org/10.1617/s11527-014-0470-9.
[14] Tetta ZC, Koutas LN, Bournas DA. Textile-reinforced mortar (TRM) versus fiber-reinforced polymers (FRP) in shear strengthening of concrete beams. Compos Part B 2015;77:338–48. http://dx.doi.org/10.1016/j.compositesb.2015.03.055.
[15] Loreto G, Babaeidarabad S, Leardini L, Nanni A. RC beams shear-strengthened

with fabric-reinforced-cementitious-matrix (FRCM) composite. Int J Adv Struct Eng (IJASE) 2015:1–12.
[16] Ombres L. Structural performances of reinforced concrete beams strengthened in shear with a cement based fiber composite material. Comp Struct 2015;122:316–29.
[17] Trapko T, Urbańska D, Kamiński M. Shear strengthening of reinforced concrete beams with PBO-FRCM composites. Compos Part B 2015;80:63–72.
[18] Koutas LN, Pitytzogia A, Triantafillou TC, Bousias SN. Strengthening of infilled reinforced concrete frames with TRM: study on the development and testing of textile-based anchors. J Compos Constr 2014;18(3). http://dx.doi.org/10.1061/(ASCE)CC.1943-5614.0000390.
[19] 1015-11 EN. Methods of test for mortar for masonry – Part 11: determination of flexural and compressive strength of hardened mortar. Brussels: Comité Européen de Normalisation; 1993.
[20] Koutas L, Triantafillou TC. Use of anchors in shear strengthening of reinforced concrete T-beams with FRP. J Comp Constr 2013;17(1):101–7.
[21] Bournas DA, Pavese A, Tizani W. Tensile capacity of FRP anchors in connecting FRP and TRM sheets to concrete. Engin Struct 2015;82(1):72–81.
[22] Ozbakkaloglu T, Saatcioglu M. Tensile behavior of FRP anchors in concrete. J Comp Constr 2009;13(2):82–92. 82.
[23] ACI Committee 440. Guide test methods for fiber-reinforced polymers (FRPs) for reinforcing or strengthening concrete structures (ACI 440.3R-04). Farmington Hills, MI: American Concrete Institute; 2004. p. 40.
[24] Pellegrino C, Vasic M. Assessment of design procedures for the use of externally bonded FRP composites in shear strengthening of reinforced concrete beams. Compos Part B 2013;45(1):727–41.
[25] Rousakis T, Saridaki M, Mavrothalassitou S, Hui D. Utilization of hybrid approach towards advanced database of concrete beams strengthened in shear with FRPs. Compos Part B 2016;85:315–35.